

Emission from dielectric cavities in terms of invariant sets of the chaotic ray dynamics

Eduardo G. Altmann*

Northwestern Institute on Complex Systems, Northwestern University, 60628 Evanston, IL, USA

In this paper, the chaotic ray dynamics inside dielectric cavities is described by the properties of an invariant chaotic saddle. I show that the localization of the far field emission in specific directions is related to the filamentary pattern of the saddle's unstable manifold, along which the energy inside the cavity is distributed. For cavities with mixed phase space, the chaotic saddle is divided in hyperbolic and non-hyperbolic components, related, respectively, to the intermediate exponential ($t < t_c$) and the asymptotic power-law ($t > t_c$) decay of the energy inside the cavity. The alignment of the manifolds of the two components of the saddle explains why even if the energy concentration inside the cavity dramatically changes from $t < t_c$ to $t > t_c$, the far field emission changes only slightly. Simulations in the annular billiard confirm and illustrate the predictions.

PACS numbers: 42.15.-i, 05.45.-a

I. INTRODUCTION

Motivated by technological applications, the emission from dielectric microcavities of different shapes has been the focus of detailed experimental investigations [1, 2, 3, 4] and wave simulations [5, 6, 7, 8, 9, 10, 11, 12]. Comparisons between the measurements and the predictions of the (chaotic) ray dynamics reveal an overall good agreement, including detailed properties of the far-field emission [7, 8, 9, 12]. These recent results renew the interest on the classical/ray dynamics in open chaotic systems *per se*, i.e., not only as the short-wavelength limit of the quantum/wave description [13, 14, 15, 16, 17].

The ray dynamics inside dielectric cavities is determined by the laws of geometric optics: rays travel in straight lines between collisions at the boundary of the cavity, where they generically split in reflected and transmitted (refracted) rays with intensities given by Fresnel's law. Far field emissions peaked in specific directions have been surprisingly observed even in cavities where the reflected rays have (uniformly) chaotic dynamics [1, 2, 3, 4, 5, 7, 12, 18]. Directionality in the far field and good confinement (high Q modes) are requirements for applications of microcavities as lasing systems [1]. The following two recent results have proved to be crucial for a ray description of the far field emission: (i) Lee *et al.* [6] introduced the *survival probability distribution* of the intensities of rays inside the cavity. In strongly chaotic systems, this distribution decays exponentially in time and numerical evidence was presented for a steady phase-space dependence of the probability distribution, independent of initial conditions (see Ref. [19] for a detailed description, and also Refs [6, 8, 9, 10, 16]). (ii) Schwefel *et al.* [7] explained the observation of peaked far-field intensities by relating the regions of high emission to the unstable manifold of periodic orbits close to the boundary of the region of total internal reflection.

This has been further investigated in Refs. [8, 9, 12].

In this paper, the ray dynamics in dielectric cavities is described using the ergodic theory of transient chaos [20, 21, 22, 23]. After properly taking into account the *partial* leak characteristic of dielectric cavities, the long-time properties of the chaotic dynamics are governed by an invariant set of the classical dynamics, the so called *chaotic saddle* (CS), composed by all trajectories that never leave the cavity in both forward and backward times. This provides an unified and more general treatment of the results (i) and (ii) mentioned above: (i) the steady survival probability distribution introduced by Lee *et al.* in [6], is equivalent to the conditionally invariant density ρ_c [24, 25, 26]; and (ii) the emission pattern is governed by the unstable manifold of the CS (not only of a single periodic orbit) along which the measure concentrates [25]. The importance of the CS and its manifolds has been recently recognized in the computation of the distribution of resonances [14, 16] and as the origin of a fractal Weyl's law [13, 15]. This paper, instead, focus on the importance of the CS in the *classical* ray dynamics inside dielectric cavities and how the main physical properties (decay rate γ , emission pattern) can be obtained from it. Furthermore, I argue how to extend these results to the case of generic cavities, where regions of regular and chaotic motion coexist in a *mixed phase space*. In particular, I show how a division of the CS in a hyperbolic and a non-hyperbolic component [27, 28, 29] explains why even if the concentration of energy inside the cavity changes in time, the far field emission retains its main properties.

The paper is divided as follows. In Sec. II the classical ray dynamics and the standard description in terms of the chaotic saddle is presented. The case of systems with mixed phase space is considered in Sec. III. Sec. IV presents numerical simulations on the annular billiard. Finally, the main conclusions are summarized in Sec. V

*Electronic address: ega@northwestern.edu

II. CHAOTIC RAY DYNAMICS IN DIELECTRIC CAVITIES

A. Classical ray dynamics

Rays inside a dielectric cavity travel in straight lines between successive collisions at the cavity's boundary, where the ray generically splits in a reflected and a transmitted (or refracted) ray. The direction of propagation of the rays are determined by the angle in respect to the boundary's normal vector at the collision point. The reflected angle $\theta_R \equiv \theta$ is equal to the incident angle θ_I , while the transmitted angle θ_T is given by Snell's law as $\sin \theta_T = n \sin \theta_I$, where n is the ratio between the (constant) refractive indices in- and out-side of the cavity. The intensities of the rays after collision are given by Fresnel's law and total internal reflection occurs for $p \equiv \sin \theta_I > \sin \theta_c = 1/n \equiv p_c$. These are the well established laws of geometric optics.

Assuming the validity of geometric optics, the dynamics of a ray is defined exclusively by its initial condition and the geometry of the cavities boundary (parametrized by s). For simplicity, let us consider the case of two dimensional cavities or billiards (the main results below remain valid for the three-dimensional case). The boundary's geometry defines a function M that maps one collision to the next $M : (s_t, p_t) \mapsto (s_{t+1}, p_{t+1})$. M preserves the area $d\mu = dsdp = d\sin \theta$, what establishes the analogy to Hamiltonian systems. Below, I focus on the dynamics of maps M that have at least one chaotic component. The discrete time t can be related to the actual time using the mean time between bounces $\pi A/Sc$ where A is the area of the billiard, S is the perimeter, and c is the speed of the ray. This is an approximation for individual rays [30].

The above picture describes the dynamics in closed billiards. In order to introduce the escape through the transmitted rays (according to Snell's and Fresnel's laws), we consider that each ray has an intensity i , with $i_{t=0} = 1$. After each collision the intensity of the reflected ray i_{t+1} depends on i_t , the angle θ_I and on the polarization of the incident ray. For transverse magnetic (TM) and transverse electric (TE) polarization Fresnel's law gives

$$\begin{aligned} R_{TM}(\theta) &= \left[\frac{\sin(\theta_T - \theta_I)}{\sin(\theta_T + \theta_I)} \right]^2, \\ R_{TE}(\theta) &= \left[\frac{\tan(\theta_T - \theta_I)}{\tan(\theta_T + \theta_I)} \right]^2, \end{aligned} \quad (1)$$

for $|\sin(\theta_I)| < 1/n = p_c$ and $R = 1$ otherwise (total internal reflection). The transmitted rays have angle θ_T and intensity $T = 1 - R$. The region of the phase space $-p_c < p < p_c$ (where $T > 0$) will be denoted as *leak region I*.

In summary, the full ray dynamics is given by $(s_t, p_t, i_t) \mapsto (s_{t+1}, p_{t+1}, i_{t+1})$, where $M : (s_t, p_t) \mapsto (s_{t+1}, p_{t+1})$ is an area preserving map defined by the geometry of the billiard and the intensity $i_{t+1} = R(p)i_t$

decreases in time according to Fresnel's law (1). The energy in one region Ω of the phase space at time t is given by the intensities i_t and density $\rho(s, p, t)$ of rays inside it:

$$E((s, p) \in \Omega, t) = \int_{\Omega} \int_{\Omega} i(s, p, t) \rho(s, p, t) ds dp. \quad (2)$$

The direction, position, and intensity of the rays emitted from the cavity can be computed by Fresnel's and Snell's law from $E(s, p, t)$ inside I .

B. Estimations based on the closed system

Let us first consider the case of billiards where the dynamics of the closed map M is strongly chaotic (e.g., uniformly hyperbolic) [22], leaving the generic case of systems with mixed phase space for Secs. III and IV. For strongly chaotic systems, after a short transient time t^* the fraction of rays that never entered I decays exponentially [28]. The intensity i decreases with successive bounces inside I , and rays in I return typically exponentially fast to it. Therefore, the total energy inside the cavity $E(t)$ decays also exponentially. This means a constant leakage rate r (transmitted energy per unit of time). It follows that (2) is given by [22]

$$E(t) \sim (1 - r)^t = \exp[\ln(1 - r)t],$$

and the escape rate γ corresponds to

$$\gamma = -\ln(1 - r) \quad [\approx r \text{ for small } r]. \quad (3)$$

Let us assume now that the closed system is ergodic, i.e., it can not be divided in two regions A and B with $\mu(A) > 0$ and $\mu(B) > 0$. In this case, and when the leak I is small, one can estimate the leakage rate r using the natural measure of the *closed* billiard as

$$r^* \approx r_{\mu} = \int_I T(\theta) d\mu = \int_0^1 \int_{-\theta_c}^{+\theta_c} [1 - R(\theta)] \cos \theta d\theta ds. \quad (4)$$

The leakage rate r was called *degree of leakage* in Ref. [19] where analytical expressions for (4), using R_{TM} and R_{TE} given by (1), were obtained. They show the interesting dependency $r \sim 1/n^2$ that was verified numerically. Similarly, the ray dynamics described above has been successfully applied in cavities with different shapes [1, 2, 3, 4, 5, 6, 7, 8, 9, 10, 11, 12]. It is interesting to compare these applications in optics to previous investigations involving other leaked systems [24, 28, 31, 32, 33, 34, 35]. The main difference is the *partial* leak through Fresnel's law in the optical systems (also present in acoustics [30]), in opposition to a complete escape assumed in the previous cases. However, as we will see below, once the intensity of the rays is properly taken into account, a complete correspondence can be established. For instance, relation (4) is a standard estimation [21, 22, 23]. Dependence on the position of I has been reported [32, 33] and, as expected, Eq. (4)

is strictly valid only in the limit of $r \rightarrow 0$, what is of little practical interest for optical systems since it corresponds to $n \rightarrow \infty$. However, it is important to note that approximations based on the closed system properties are, in some cases, the only available and that they can lead to successful predictions [2]. In the next section, I take further profit from the analogy to leaked systems to apply fundamental results of the ergodic theory of transient chaos (and chaotic scattering) to obtain a description of ray dynamics in *open* optical cavities.

C. Description in terms of invariant sets of the open system

Transient chaotic motion is typical for leaked systems and naturally open systems showing chaotic scattering [20, 21, 22, 23]. The escape of trajectories that remain a long time inside the system is described by an invariant, non-attracting, chaotic set [20, 21, 22, 23]. This set is composed by the trajectories that never leave the system, neither in forward nor in backward iterations of the map. The stable (unstable) manifold of this set is defined by all points that lead to this set in forward (backward) time. The term *chaotic repeller* is sometimes used to denote this set [12, 15, 16, 20, 21]. Because in billiards the dynamics is time reversible, having therefore stable and unstable manifolds, the term *chaotic saddle* (CS) is adopted in this paper [23, 25]. For strongly chaotic ergodic systems, the CS has zero Lebesgue measure $\mu(CS) = 0$ (vanishing area of the phase space), and the support of the CS is a fractal set. The stable and unstable manifolds cross orthogonally (angle bounded from zero) and are also of zero Lebesgue measure. Trajectories that survive for a long time inside the system necessarily have initial conditions close to the stable manifold of the CS, approach closely the CS, and leave the system through the unstable manifold of the CS. A well defined escape rate γ exists which is independent of the density of initial conditions ρ_0 , provided it intersects the stable manifold of the CS. Relations between γ and the properties of the CS (fractal dimension along the manifolds, Lyapunov exponent) have been previously derived [21, 22, 23].

Let us see now how these results can be adapted to the case of optical cavities, where the leakage is only partial inside I and the dynamics involves not only the map M but also the decay of the intensity i . A natural definition of the CS is obtained replacing the condition of never escaping trajectories mentioned above by the condition that $i = 1$ for all times:

$$(p_{CS}, s_{CS}) \in CS \Leftrightarrow i(p_{CS}, s_{CS}, t \rightarrow \pm\infty) = 1. \quad (5)$$

In other words, the CS of the leaked system defined by (5) is the same obtained considering a full leak and the standard definition of the saddle, i.e., replacing the partial leak in (1) by a Heaviside step function. It follows that: $CS \cap I = \emptyset$. A definition similar to (5) is not appropriate

for the manifolds of the CS. For instance, initial condition inside I that converge to the CS for $t \rightarrow \infty$ and still have $i_{t \rightarrow \infty} \neq 0$ clearly deserve to belong to the saddle's stable manifold (similar argument for $t \rightarrow -\infty$ holds for the unstable manifold). The stable (unstable) manifold of the CS is therefore defined by *all* points $(s, p) \rightarrow CS$ for $t \rightarrow +\infty$ ($-\infty$), but attached to these points there is a manifold intensity i given by $i_{t \rightarrow \infty}$ ($i_{t \rightarrow -\infty}$). This suggests an alternative definition for the CS itself:

$$(p_{CS}, s_{CS}) \in CS \Leftrightarrow i(p_{CS}, s_{CS}, t \rightarrow \pm\infty) > 0. \quad (6)$$

The CS defined using (6) contains the CS defined using (5): $CS(5) \subset CS(6)$. Moreover, all points outside of: $CS(6) \cap CS(5)$, collide only a finite number of times inside I and necessarily belong to the intersection of the stable and unstable manifolds of CS(5). Therefore, for long times, all rays with non-vanishing intensities inside the cavity will be governed by the CS (5) and its manifolds. This justifies the choice of relation (5) and shows that this CS also governs the decay of energy from the billiard.

With the above definitions of the invariant sets, let us characterize the escape from the cavity. The proper measure to describe this decay is the conditionally invariant measure (c measure) $d\mu_c$ [24, 25, 26]. Intuitively, the mathematically well defined c measure is obtained multiplying the survival density by a factor proportional to $\exp(\gamma t)$ that compensates the decay of the Lebesgue measure [28]. The conditionally invariant density ρ_c concentrates along the unstable manifold of the CS [25] and is the only attractor for typical initial densities ρ_0 [24, 26]. The leakage rate r , that determines the decay rate γ through (3), is precisely given by the c measure of the leak I [24, 28]

$$r = \int_I T(\theta) d\mu_c = \int_0^1 \int_{-\theta_c}^{+\theta_c} [1 - R(\theta)] \rho_c(\theta, s) \cos\theta d\theta ds. \quad (7)$$

An important property of the c measure is that it converges to the natural measure for $\mu(I) \rightarrow 0$ [24, 26]. This implies that r^* in (7) is equivalent to r in (4) for small I (large n). Typically r^* overestimates r [29].

It is remarkable that many of the results presented above have been recently rediscovered in the analysis of optical cavities. For instance, the steady state of the survival probability distribution, introduced by Lee *et al.* [6] and mentioned as point (i) in the introduction above, is equivalent to the conditionally invariant density ρ_c introduced by Pianigiani and York thirty years ago [24] (see Ref. [26] for a recent review). The independence of initial ensembles reported in Ref. [6] is related to the existence of the invariant CS or, equivalently, to the fact that ρ_c is the only attractor for typical ρ_0 's. The density ρ_c concentrates along the unstable manifold of the CS [25], which presents the characteristic filamentary pattern inside I . This explains the peaked distribution of the transmitted rays responsible for the emission from the cavity. When a short time periodic orbit exists close to the critical

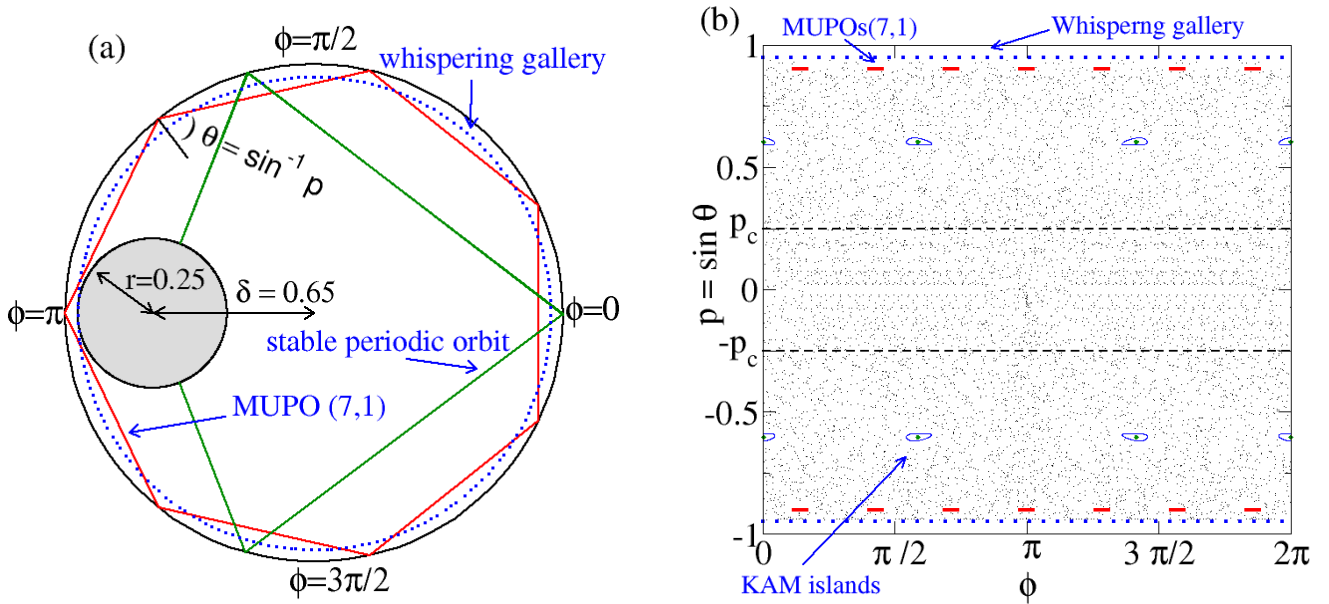


FIG. 1: (Color Online) (a) Annular billiard defined by two concentric circles, with control parameters $r = 0.65$ and $\delta = 0.3$. Lines indicate one stable periodic orbit (at $\phi = 0$) and one MUPO (7,1) (polygonal form) [37]. Trajectories that do not cross the dotted circumference of radius $r + \delta$ belong to the whispering gallery. (b) Phase space representation of the closed billiard shown in (a), obtained using a Poincaré surface of section at the outer boundary (parametrized by $s = \phi \in [0, 2\pi]$). The stable periodic orbit in (a) is at the center of a chain of KAM islands. Black dots mark 8000 iterations of single chaotic trajectory. The horizontal dashed lines denote $p_c = \pm 1/n$ for $n = 4$, as used in the following figures.

line $p = p_c$, the unstable manifold of this orbit (which also belongs to the CS) will be parallel to the manifold of the remaining part of the CS (both manifolds do not intersect). This corresponds to the observation by Schwefel *et al.* [7] described as point (ii) in the introduction above.

III. SYSTEMS WITH MIXED PHASE SPACE

The results described so far can be rigorously applied only for a limited class of strongly chaotic systems. It can be argued that it is a technical problem to extend these demonstrations to a larger class of non-uniform hyperbolic systems, where no deviation of the exponential decay has been numerically detected. However, cavities with generic boundaries have typically a mixed phase space: coexisting with regions of chaotic motion there are regions of regular motion, e.g., Kolmogorov-Arnold-Moser (KAM) islands. Around these regions there is a *sticky region* where chaotic trajectories get partially trapped, introducing a power-law like decay of the survival probability. Rigorously, the results of the theory of transient chaos mentioned above either do not apply or become trivial. This type of cavities have been considered in Refs. [3, 5, 7] and without further justifications it is not clear how the previous results can be extended to this case.

In this section, I show how, despite the mathematical difficulties, in practice the formalism of the CS and its

manifolds can be applied to billiards presenting a divided phase space. The basic observation is that typically a well defined exponential decay of the survival probability exists for intermediate times, where in practice the previous results can be applied [27, 28]. I am interested in the case of billiards containing a large chaotic component and in the escape of energy from this component. I restrict also to the case where KAM islands are not present in the border of I . In this case, similar to the decay of particles, the decay of energy (2) shows a transition from exponential to asymptotic power-law [19, 28, 31, 34, 35, 36]

$$E(t) = \begin{cases} Ae^{-\gamma t} & \text{for } t > t^*, \\ Ae^{-\gamma t} + Bt^{-\alpha} & \text{for } t > t_\alpha, \end{cases} \quad (8)$$

where t^* is proportional to the inverse of the negative Lyapunov exponent of the saddle, t_α is the shortest time rays in the sticky region need to reach I , and $Ae^{-\gamma t_\alpha} \gg Bt_\alpha^{-\alpha}$. The transition time $t_c > t_\alpha$ between the exponential and power-law decays in (8) is defined as $Ae^{-\gamma t_c} = Bt_c^{-\alpha} = E(t_c)/2$, i.e., for $t > t_c$ the power-law decay dominates. In Ref. [28] it was shown that $t_c \sim 1/\gamma$ and suggested that exponential and power-law regimes in (8) can be related, respectively, to hyperbolic and non-hyperbolic components of the CS, as first suggested in [27]. The non-hyperbolic component consists of the border of KAM islands (and by other marginal stable orbits) while the hyperbolic part is away of the sticky regions and resembles the CS described in Sec. IV C. Initial conditions uniformly distributed (i.e.,

touching the KAM islands) modify the exponent α in Eq. (8) [36]. Because (8) is a survival probability distribution, typically $0 < \alpha \leq 1$. The exact (finite time) value depends on the properties of the non-hyperbolic region (KAM island).

In terms of the energy inside the cavity, Eq. (8) indicates that while for $t < t_c$ energy concentrates strongly in the hyperbolic component of the CS and its manifolds, for $t > t_c$ the energy concentrates in the non-hyperbolic component of the CS. In principle, one could expect also a dramatic change in the emission pattern from $t < t_c$ to $t > t_c$. However, as emphasized in Ref. [28], an important difference between the hyperbolic and non-hyperbolic components of the CS is that their manifolds attract and repel exponentially and sub-exponentially respectively. Therefore rays approach and escape slowly the non-hyperbolic component of the CS *through* the hyperbolic component. In particular, when KAM islands are away from I , before escaping rays will meet the stable/unstable manifolds of the *hyperbolic* component of the CS that will control their escape. In other words, the unstable manifold of the non-hyperbolic component of the CS align to the unstable manifold of the hyperbolic component of the CS. From this picture we expect that, even if the density concentrates for long times $t > t_c$ on the non-hyperbolic component of the CS, the decay towards I will still follow the manifold of the hyperbolic component of the CS and, therefore, do not dramatically differ between $t < t_c$ and $t > t_c$. This prediction is partially confirmed in the next Section, when numerical simulations of a specific system are presented.

IV. NUMERICAL SIMULATIONS

A. The annular billiard

Numerical simulations of the ray dynamics are performed in the annular billiard depicted in Fig. 1a. The closed phase space shown in Fig. 1b shows a large chaotic sea coexisting with three regions of regular dynamics: the chain of KAM islands and two whispering gallery regions close to the outer boundary. Whispering gallery regions are typical for billiards with concave shape [4, 5, 12]. In the case of the annular billiard an infinite number of families of marginally unstable periodic orbits (MUPOs) accumulate outside of the whispering gallery [37], where to the chaotic trajectories stick with $\alpha = 1$ in Eq. (8) [36].

B. Time dependency

Consider now that the larger circle in the annular billiard (Fig. 1a) has refractive index n , the outside space $n = 1$, and the boundary of the inner circle is a perfect mirror. In this case, emission according to (1) is possible through the outer border when $|p| < |p_c| = 1/n$, i.e., the leak region I corresponds to an horizontal stripe

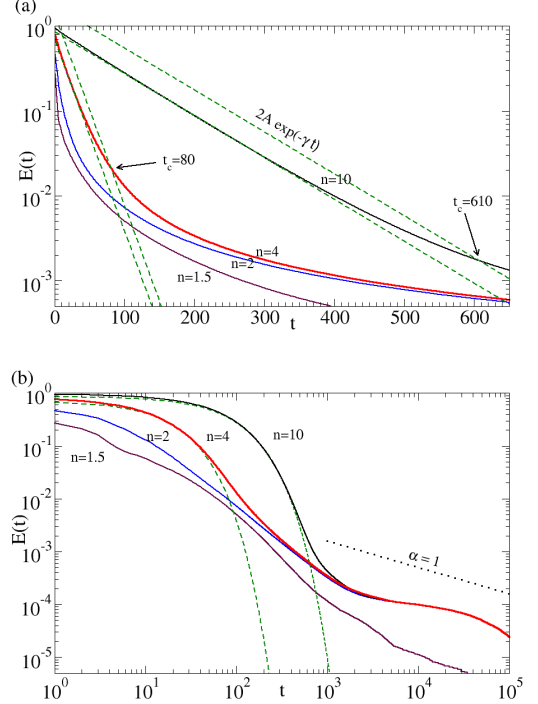


FIG. 2: (Color online) Energy inside the annular billiard shown in Fig. 1 for $n = \{10, 4, 2, 1.5\}$ (from top to bottom). (a) linear-log and (b) log-log scale. The dashed lines correspond to an exponential fitting for short times and t_c indicates the transition time to a power-law. Rays were started uniformly distributed in the chaotic component.

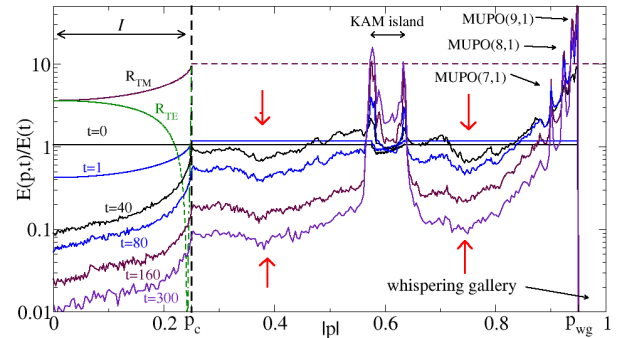


FIG. 3: (Color online) Energy along p at time t normalized by total energy at time t , for $t = 0, 1, 40, 80, 160$, and 300 (top to bottom). Refractive index $n = 4$ leads to $p_c = 0.25$ and $t_c = 80$ (see Fig. 2). Rays were started uniformly distributed in the chaotic component (*outside* the KAM island). Vertical arrows indicate minima of the distribution that systematic appear for all times. Dashed lines indicates the reflection coefficient R in Eq. (1), multiplied by 10 for clarity.

between $-p_c < p < p_c$ in the center of the phase space shown in Fig. 1(b). Typically, 10^7 TM polarized rays (similar results are expected for TE) are started inside the chaotic component uniformly distributed according to the Lebesgue measure (area of the phase space). This means that no rays are started inside the KAM island

or whispering gallery. The temporal decay of the total energy is presented in Fig. 2 for different values of the refractive index n . It confirms the existence of an intermediate exponential decay and an asymptotic power-law decay, as described by Eq. (8). Different exponents can be identified for $n = 2$ and 4: $1 < \alpha \leq 2$ for intermediate times, related to rays that approach the KAM island (started away from it), and $0 < \alpha \leq 1$ related to rays started already close to the KAM islands. For $n = 2, 4$, and 10 the energy decay converges precisely. Hereafter the representative case $n = 4$ is chosen, for which the generic exponential and power-law decays are clearly visible in Fig. 1 and $t_c = 80$.

Let us see now how the energy is distributed inside the billiard at a given time t . Figure 3 shows the distribution projected to the p axis for different times t . The total energy in all cases is normalized and the rays are started uniformly in the chaotic component. For fully chaotic system this distribution converges to the conditionally invariant density ρ_c (see Sec. III). Instead, Fig. 3 shows a concentration of the energy close to the KAM island and whispering gallery. This is a consequence of the power-law escape of rays in these sticky regions, in opposition to the exponential escape for rays away from these regions. Apart from a rescale due to this decay, Fig. 3 suggests that also the distribution away from islands follows a similar pattern (see, e.g., the vertical arrows in Fig. 3) for all times $t < t_c$ and $t > t_c$. This is in agreement with the interpretation given at the end of Sec. III and will be further investigated below.

C. Chaotic saddle

In this section we will see how the division of the chaotic saddle in hyperbolic and non-hyperbolic components proposed in Sec. III apply for the annular billiard considered here. The non-hyperbolic component of the CS is composed by the border of the KAM islands, the border of the whispering gallery, and the families of MUPOs. Figure 3 shows that the energy concentrates in this region for long times. Regarding the hyperbolic component, a simple and efficient method to obtain a visualization of this zero measure set was proposed in Ref. [23] (page 201). It is based on the observation that (most) trajectories that survive until some long time t^\dagger were close to the stable manifold of the CS at time $t = 0$, were close to the CS at time $t = t^\dagger/2$, and were close to the unstable manifold at time $t = t^\dagger$. This method is expected to work for the hyperbolic component of the CS if $t^* \ll t^\dagger < t_c$ and if initial conditions are selected away from sticky regions, i.e., *non-uniformly* in the chaotic sea. The results achieved for the annular billiard are shown in Fig. 4, where only components of the unstable manifold with $i > 0.01$ are plotted.

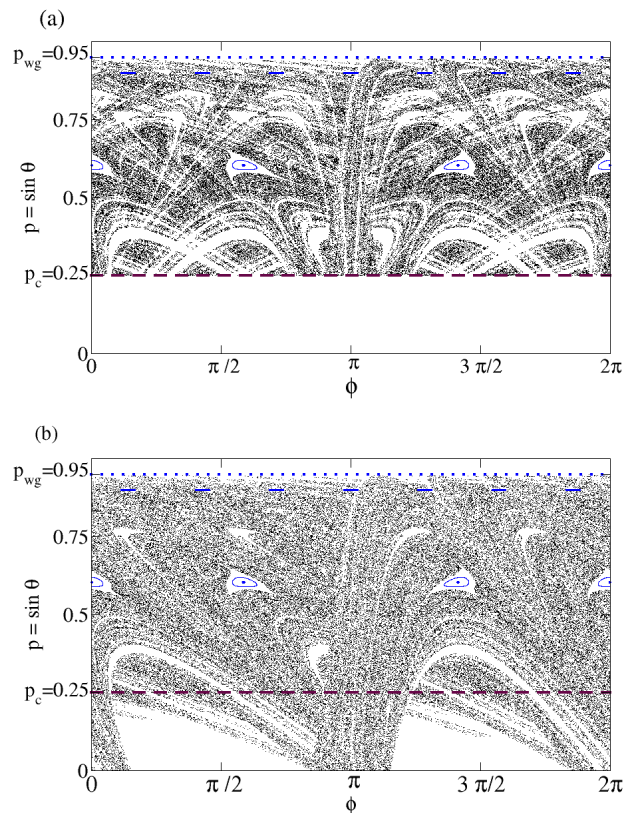


FIG. 4: (Color online) (a) Hyperbolic component of the CS and (b) its unstable manifold for $n = 4$. Method of Ref. [23] with $t^\dagger = 30 < t_c = 80$ was employed, with rays started *non-uniformly* outside the regions of regular motion. Only points with $i > 0.01$ are plotted in (b). Due to the time reversible symmetry and the spatial symmetry of the annular billiard, the stable manifold of the CS can be obtained from the unstable one by $(s, p) \mapsto (2\pi - s, p)$.

D. Energy distribution and emission

Finally, the distribution of energy inside the cavity and the far field emission are investigated. Considering the time dependency obtained in Sec. IV B, where $t_c = 80$ was found for $n = 4$, two times are considered: $t = t_c/2 = 40$, for which the decay is exponential and the hyperbolic component of the CS dominates, and $t = 2t_c = 160$, for which the decay is algebraic and the non-hyperbolic component of the CS dominates. The relative distribution of energy at these times are expected to be representative for all times in the exponential and power-law decays (e.g., the relative distribution for $t \rightarrow \infty$ is expected to resemble the one at $t = 160$). The numerical results are shown in Fig. 5. The two figures in the upper row confirm that the energy shifts from the hyperbolic component of the CS and its unstable manifold, to the non-hyperbolic component of the saddle. The two figures in the lower row are amplifications of the upper figures in the leak region, which is the relevant region for emission

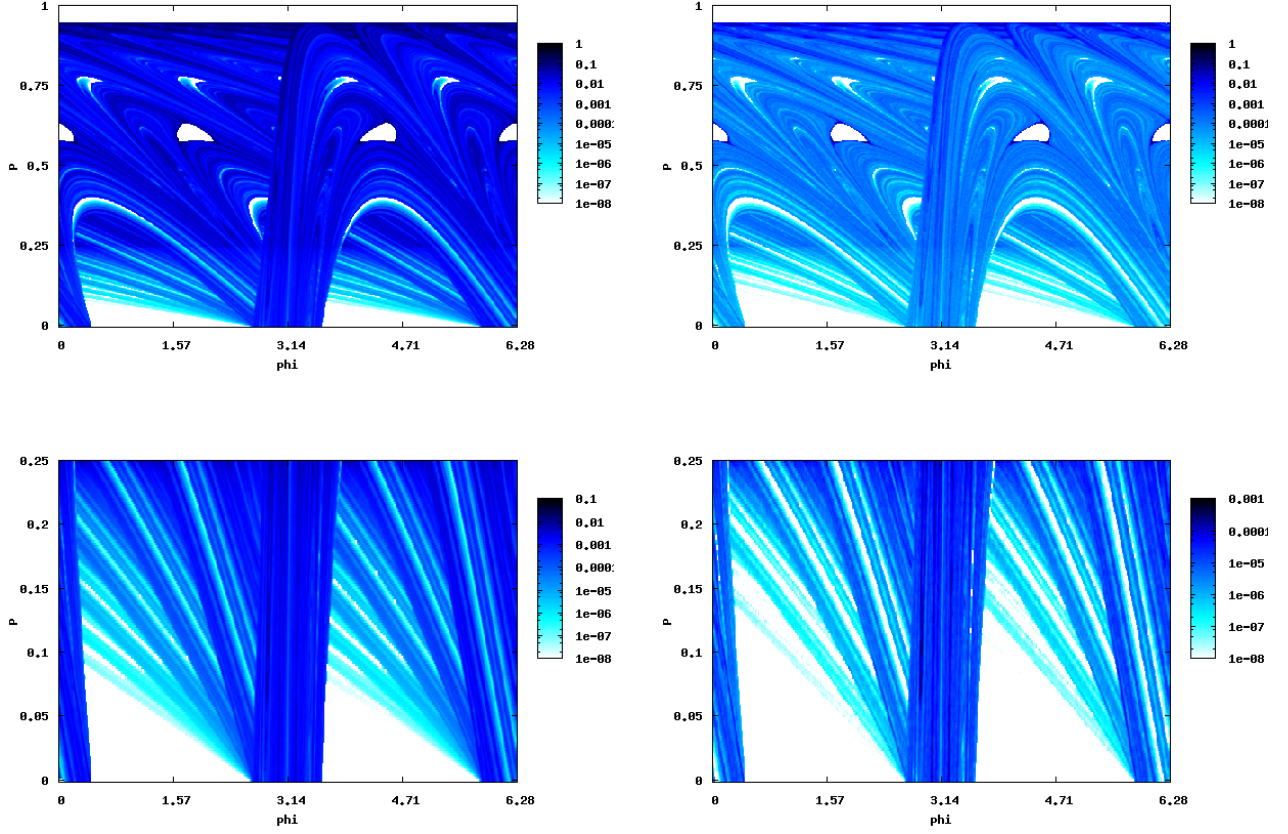


FIG. 5: (Color online) Distribution of energy in the phase space of the annular billiard for $n = 4$ ($p_c = 0.25$) at two different times: Left $t = 40 = t_c/2$; Right $t = 160 = 2t_c$. Bottom row shows an amplification of the top row in the leak region. Rays were started uniformly distributed in the chaotic region.

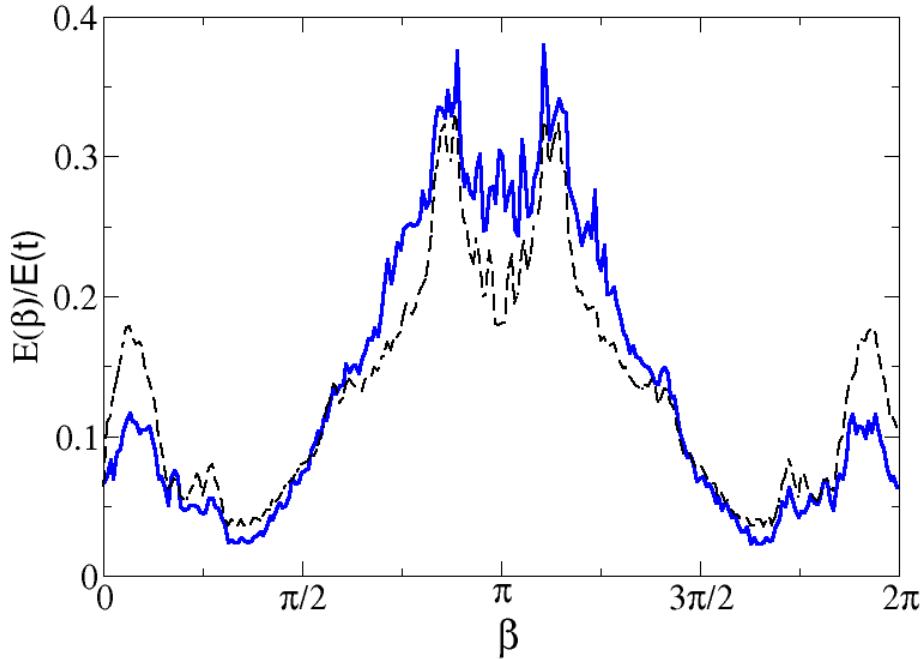


FIG. 6: (Color online) Far field intensity transmitted in the direction $\beta = \phi - \theta_T$ measured from the center of the annular billiard at times $t = t_c/2 = 40$ (dashed line) and $t = 2t_c = 160$ (solid line). Rays were started uniformly distributed in the chaotic region and $n = 4$.

purposes. The differences between $t = 40$ and $t = 160$ are much less dramatic in this case. Comparing to Fig. 4b, we see that the energy is non-vanishing along the unstable manifold of the (hyperbolic component of) the CS, and only the relative intensity is (slightly) changed in time. This different intensities is enough to change the far-field emission as shown in Fig. 6. An overall similar pattern is observed for both times, but with different intensities at different emission angles. These results are in agreement with the interpretation at the end of Sec. III that the escape from the non-hyperbolic component of the CS follow also closely the unstable manifold of the hyperbolic component of the CS. However, the numerical simulations presented here suggests that differences in the intensity inside I lead to far field emissions that are similar but not identical for $t < t_c$ and $t > t_c$.

V. CONCLUSIONS

This paper presents a description of the chaotic ray dynamics in dielectric cavities in terms of the theory of transient chaos. After properly taking into account the partial leakage introduced by Fresnel's law, the long time escape and emission are found to be governed by a chaotic saddle (CS) [20, 21, 22, 23]. The energy inside the cavity is distributed according to the c measure [24], that is non-zero along the unstable manifold of the CS [25]. In the generic case of cavities showing mixed phase space, it is useful to consider a division of the CS in an hyperbolic and non-hyperbolic components [27, 28], related to the exponential ($t < t_c$) and power-law ($t > t_c$) decays of energy inside the cavity. For longer times ($t > t_c$) the energy concentrates in the non-hyperbolic component of the CS, but the emission shows only small differences from shorter times ($t < t_c$). This is explained by the fact that, when the non-hyperbolic regions are away from the critical line, the escape from the non-hyperbolic saddle occurs mainly through the unstable manifold of the hyperbolic component.

From the point of view of previous investigations in dielectric cavities, these results provides an unifying and more general description of experiments and simulations. For instance, the localization in the far field emission is shown here to be related to the unstable manifold of the CS and not of a single periodic orbit as previously re-

ported, what is expected to be of practical relevance in cases where no low periodic orbit exists close to the critical line. From the point of view of dynamical systems theory, these results emphasize the importance of a rigorous treatment of non-hyperbolic systems and the division of the chaotic saddle in hyperbolic and non-hyperbolic components. Moreover, it is interesting to see that many of its fundamental theoretical concepts (e.g., the CS, its unstable manifolds, and c measure) achieve an experimental concreteness in optical systems. This is perhaps only comparable to the case of fluid dynamics, where the unstable manifold of the CS can be visually observed in scattering systems, specially when a constant injection or activity of tracers compensate the natural decay through the fluid flow [27, 33, 38].

Similar to the case of fluids, experiments and applications in dielectric microcavities are rarely a simple decay of rays that have been excited at some time $t = 0$, as considered in the model of this paper. Instead, energy is constantly pumped to the system from outside through some gain in the medium. The relevance of the rays that survive for long time inside the cavity, or similarly the high Q modes, is that these are the rays whose intensities are enhanced through the input of energy. The details of these mechanisms, and how they could be included in a ray picture, are beyond the scope of this paper. However, generally one can think that these different mechanisms translate in a minimum confinement time t_G , and only rays confined for times beyond t_G are relevant. In this picture, the results of this paper suggest that depending whether $t_G < t_c$ or $t_G > t_c$ the energy inside the chaotic component of the cavity changes dramatically: it will be concentrated mainly in the hyperbolic ($t_G < t_c$) or non-hyperbolic ($t_G > t_c$) component of the saddle (in optical microcavities $t_G \gg t_c$). However, the emission pattern is similar in these two cases because it is determined by the unstable manifold of the hyperbolic component of the CS inside I . The same is true if the relevant modes are *inside* the KAM islands and tunnel the (dynamical) barrier that separates them from the chaotic sea.

Acknowledgments

I thank M. Hentschel and T. Tél for illuminating discussions.

-
- [1] C. Gmachl *et al.*, Science **280**, 1556 (1998).
 - [2] M. Lebental, J. S. Lauret, J. Zyss, C. Schmit, and E. Bogomolny, Phys. Rev. A **75**, 033806 (2007).
 - [3] S.-B. Lee *et al.*, Phys. Rev. A **75**, 011802(R) (2007).
 - [4] T. Tanaka, M. Hentschel, T. Fukushima, and T. Harayama, Phys. Rev. Lett. **98**, 033902 (2007).
 - [5] J. U. Nöckel and A. D. Stone, Nature **385**, 45 (1997).
 - [6] S.-Y. Lee *et al.*, Phys. Rev. Lett. **93**, 164102 (2004).
 - [7] H. G. L. Schwefel *et al.*, J. Opt. Soc. Am. B. **21**, 923 (2004).
 - [8] S.-Y. Lee, J.-W. Ryu, T.-Y. Kwon, S. Rim, and C.-M. Kim, Phys. Rev. A **72** 061801(R) (2005).
 - [9] S. Shinohara, T. Harayama, H. E. Türeci, and A. Douglas Stone, Phys. Rev. A **74** 033820 (2006).
 - [10] S. Shinohara and T. Harayama, Phys. Rev. E **75**, 036216 (2007).
 - [11] S. Shinohara, T. Fukushima, and T. Harayama, Phys. Rev. A **77**, 033807 (2008).

- [12] J. Wiersig and M. Hentschel, Phys. Rev. Lett. **100**, 033901 (2008).
- [13] W. T. Lu, S. Sridhar, and M. Zworski, Phys. Rev. Lett **91**, 154101 (2003).
- [14] J. P. Keating, M. Novaes, S. D. Prado, and M. Sieber, Phys. Rev. Lett. **97**, 150406 (2006).
- [15] J. Wiersig and J. Main, arXiv:0712.3673 (2007).
- [16] S. Nonnenmacher and E. Schenck, arXiv:0803.1075 (2008).
- [17] J. P. Keating, M. Novaes, and H. Schomerus, Phys. Rev. A **77**, 013834 (2008).
- [18] J. Wiersig and M. Hentschel, Phys. Rev. A **73** 031802(R) (2006).
- [19] Ryu et al., Phys. Rev. E **73**, 036207 (2006).
- [20] P. Gaspard, *Chaos, Scattering and Statistical Mechanics*, (Cambridge Univ. Press, Cambridge 1998).
- [21] J. R. Dorfman *An Introduction to Chaos in Nonequilibrium Statistical Mechanics*, (Cambridge Univ. Press, Cambridge 1999).
- [22] E. Ott *Chaos in dynamical systems*, (Cambridge University Press, Cambridge, 2002).
- [23] T. Tél, and M. Gruiz *Chaotic Dynamics*, (Cambridge Univ. Press, Cambridge, 2006).
- [24] G. Pianigiani and J. A. Yorke, Trans. of the American Math. Soc. **252**, 351 (1979).
- [25] T. Tél, Phys. Rev. A **36**, 1502 (1987); T. Tél, *Transient chaos*, in: *Directions in Chaos*, Vol. 2, pp. 149-221 edited by H.-B. Lin (World Scientific, Singapore, 1990).
- [26] M. F. Demers and L.-S. Young, Nonlinearity **19**, 377 (2006).
- [27] C. Jung, T. Tél, and E. Ziemniak, Chaos **3**, 555 (1993).
- [28] E. G. Altmann and T. Tél, Phys. Rev. Lett. **100** 174101 (2008).
- [29] E. G. Altmann and T. Tél, (in preparation).
- [30] F. Montessagne, O. Legrand, and D. Sornette, Chaos **3** 529 (1993).
- [31] H. Alt et al., Phys. Rev. E **53**, 2217 (1996).
- [32] V. Paar and N. Pavin, Phys. Rev. E **55**, 4112 (1997);
- [33] J. Schneider, T. Tél, and Z. Neufeld, Phys. Rev. E **66**, 066218 (2002).
- [34] Z. Liu and Y.-C. Lai, Phys. Rev. E **65**, 046204 (2002).
- [35] J. Nagler, M. Krieger, M. Linke, J. Schöнке, and J. Wiersig, Phys. Rev. E **75**, 046204 (2007).
- [36] E. G. Altmann, A. E. Motter, and H. Kantz, Phys. Rev. E **73**, 026207 (2006).
- [37] E. G. Altmann, T. Friedrich, A. E. Motter, H. Kantz, and A. Richter, Phys. Rev. E **77**, 016205 (2008).
- [38] T. Tél, A. de Moura, Celso Grebogi, and G. Károlyi, Physics Reports **413**, 91 (2005).